J. Med. Biol. Eng. (2017) 37:791–799
DOI 10.1007/s40846-017-0251-3

ORIGINAL ARTICLE

Detrended Fluctuation Analysis of Oxyhemoglobin Saturation by Pulse Oximetry in Sleep Apnea Syndrome

Chung-Ching Hua[1] · **Chung-Chieh Yu**[1]

Received: 1 July 2016 / Accepted: 14 September 2016 / Published online: 16 June 2017

Abstract Variability of oxyhemoglobin saturation during sleep has been utilized as diagnostic index for sleep apnea. This work examined the parameters of a detrended fluctuation analysis (DFA) plot created from series data for oxyhemoglobin saturation during a sleep study in 273 subjects. A novel automated algorithm was devised to measure the parameters of a DFA log–log plot that included the slopes of 4 line segments and the coordinates and angles of their intersections. The diagnostic value of the parameters was investigated by receiver operating characteristic (ROC) curves using apnea/hypopnea index (AHI) cutoff values of 5, 15, and 30. Three of the DFA plot parameters exhibited an area under the ROC curve $\geq$0.89 for all three AHI cutoff values. Principal component analysis found a surrogate variable that increased the areas under ROC curves to greater than 0.92 for all of the AHI cutoff values. The algorithm was "leave-one-out" cross-validated and validated in another 206 subjects receiving polysomnographic studies. The results demonstrate that the DFA plot of oxyhemoglobin saturation is a useful tool for screening subjects with sleep apnea.

Keywords Detrended fluctuation analysis · Obstructive sleep apnea · Oxyhemoglobin saturation

JEL code C22

✉ Chung-Ching Hua
hc2008@adm.cgmh.org.tw

[1] Department of Internal Medicine, Chang Gung Memorial Hospital, Keelung & Chang Gung University, 222 Maijin Road, Keelung 204, Taiwan

1 Introduction

Attended, in-laboratory polysomnography is the gold standard for diagnosing obstructive sleep apnea [1]. However, this method is costly and time-consuming. Nocturnal pulse oximetry is one of the methods for low-cost apnea screening [2] and has been applied with variable success to screen for and predict sleep apnea using several indices [3]. Nocturnal pulse oximetry is inexpensive, simply performed and easily interpreted [4].Various automated algorithms based on oxyhemoglobin saturation alone or including heart rate have been developed successfully to detect sleep apnea [5–14].

Acute repetitive events of apneas and hypopneas in obstructive sleep apnea may cause oxyhemoglobin desaturation, reduction of intrathoracic pressure, and arousal of the nervous system [1]. Desaturation accompanied by hypercapnia during sleep stimulates ventilation via the chemoreflex, which is highly sensitive in patients with obstructive sleep apnea [15]. Rapidly increased ventilation causes resaturation and shortens the duration of apnea and hypopnea. Consequently, records of oxyhemoglobin saturation in obstructive sleep apnea typically exhibit small irregular fluctuations.

Irregular fluctuations provide information that can be evaluated using particular probability density distributions [16]. Detrended fluctuation analysis (DFA), one of several methods to analyze variability, evaluates the overall variation of a complex system [17]. This method is useful for predicting post-myocardial infarction ventricular tachyarrhythmia [18] and mortality [19], intensive care unit stay after coronary artery bypass surgery [20], prolonged postoperative myocardial ischemia [21], survival of patients with congestive heart failure [22], and mortality in critically ill patients [23]. The DFA also has been used to

distinguish normal subjects from patients with stroke [24] or Alzheimer's disease [25].

Time series of physiologic signals are typically irregular and non-stationary (i.e., their statistical properties change with time) [26]. The DFA quantifies correlation properties of non-stationary physiological time series by subtracting local trends [27]. A crossover phenomenon associated with changes in short- and long-range correlation properties can be observed and the characteristics of this crossover differ between normal subjects and patients with heart disease [27–29]. The characteristics of crossover on the DFA plot are affected by the correlation properties of the signal, the frequency of random spikes and their amplitudes, and the presence of segments with different local behavior [30]. Because repetitive apnea and hypopnea events in obstructive sleep apnea produce spikes with variable amplitude in serial oxyhemoglobin saturation by pulse oximetry (SpO_2) data, DFA is a suitable tool for analyzing variability in SpO_2 during sleep.

This study presents an algorithm for analyzing the DFA plot of SpO_2 data obtained from polysomnography and investigates the diagnostic value of the derived parameters in obstructive sleep apnea–hypopnea syndrome (OSAHS).

2 Methods

2.1 Subjects and SpO_2 Data

A training set of 273 consecutive (from March 2004 to August 2005) subjects and a test set of another 206 consecutive (from February 2006 to August 2006) subjects suspected clinically of having sleep apnea syndrome were referred to our institution for polysomnographic evaluation. The training set had a similar distribution to the test set in age (45.8 ± 16.5 years vs. 46.2 ± 13.4 years), body-mass index (26.4 ± 5.1 vs. 27 ± 4.9), or male/female ratio (209/64 vs. 166/40), but a lower apnea/hypopnea index (AHI; 31.6 ± 27.1 vs. 44.1 ± 29.8). The details of the subjects' characteristics, methods of performing polysomnography, criteria for the diagnosis and staging of OSAHS, acquisition of SpO_2 signal, and the processing of artifactual data have been reported previously [31]. The SpO_2 signal was presented with 1 datum per second. The study was approved by the Institutional Review Board at Chang Gung Memorial Hospital.

2.2 Detrended Fluctuation Analysis

The DFA algorithm (Fig. 1) [27] was applied to SpO_2 data for each subject. Briefly, the mean of SpO_2 values was first subtracted from each data point to form a new integrated time series $y(k)$ with length N. The $y(k)$ was then divided into boxes of equal size n with lengths from 4 to 1/10 of N, which was chosen to avoid the under-sampling of $F(n)$ (see below) when n approached N [32]. In each box of n, a linear regression was applied to find a local trend, and the y coordinate of the fit line was denoted by $y_n(k)$. The integrated time series $y(k)$ was then detrended by subtracting the local trend in each box. For a given box size n, the root–mean–square fluctuation $\left(F(n) = \sqrt{\frac{1}{N}\sum_{k=1}^{N}[y(k) - y_n(k)]^2}\right)$ of the integrated time series was calculated to obtain $F(n)$. A log $F(n)$ to log n plot of DFA (Fig. 2) was constructed for further analysis.

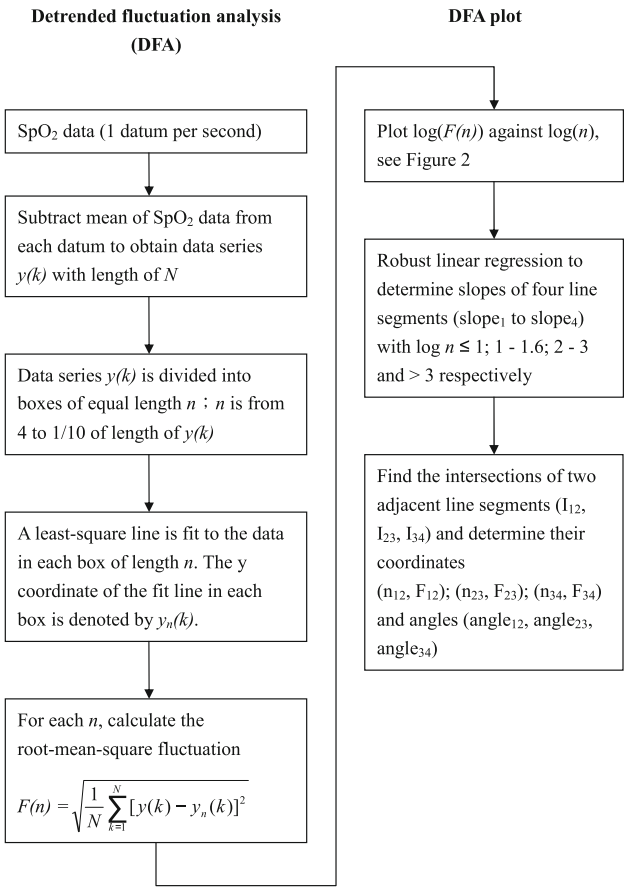

Fig. 1 Algorithms for detrended fluctuation analysis of serial oxyhemoglobin saturation by pulse oximetry (SpO_2) data and its log–log plot

2.3 Parameters of the DFA Plot

Robust linear regression with MM estimation [33] was applied to find the slopes of 4 line segments ($slope_1$–$slope_4$) with endpoints log *4* and 1; 1 and 1.6; 2 and 3; and 3 and log *N/10*, respectively (Fig. 2). The coordinates [(n_{12}, F_{12}); (n_{23}, F_{23}); (n_{34}, F_{34})] and angles ($angle_{12}$, $angle_{23}$, $angle_{34}$) of 3 intersections (I_{12}, I_{23}, I_{34}) formed by each two adjacent

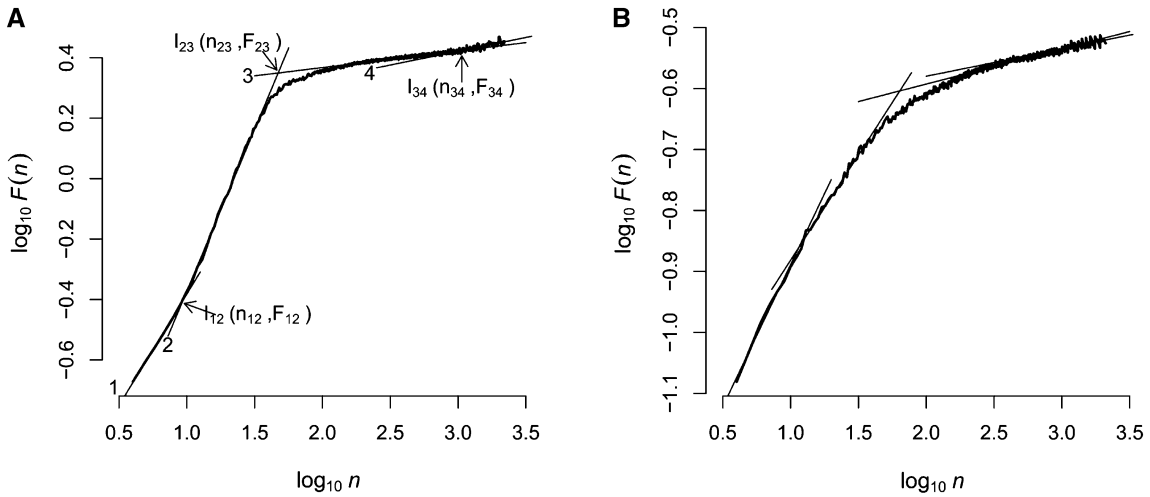

Fig. 2 **a** Detrended fluctuation analysis (DFA) plot of oxyhemoglobin saturation by pulse oximetry (SpO_2) data in a subject with severe obstructive sleep apnea with an apnea/hypopnea index (AHI) of 69.4. *Numbers* 1–4 denote the lines derived from robust linear regression of log F(n) on log n in 4 line segments with endpoints log 4 and 1; 1 and 1.6; 2 and 3; and 3 and log N/10, respectively. Subscripts of intersection (I) represent the number of two adjacent lines, and the intersection coordinates are listed in *parentheses*. A curved crossover is seen in the interval of log n between 1 and 3. **b** DFA plot of SpO_2 data in a subject with an AHI of 1.6

line segments were solved via their underlying linear equation derived from robust linear regression.

The DFA algorithm and a parameter analysis of the DFA plot were developed via the R statistical package [34].

2.4 Principal Component Analysis (PCA)

The parameters of the DFA plot were highly inter-correlated (49% with correlations significant at the 0.01 level in the training set). Variables with a measure of sampling adequacy less than 0.5 [35] or a communality less than 0.8 were deleted in a stepwise fashion and a surrogate variable (PC1) with components of $slope_2$, $angle_{23}$, F_{23}, and F_{34} was extracted from DFA plot parameters during the PCA process. The PC1 variable extracted 89.95% of variance from the original data and its score was calculated with regression coefficients of 1.738, −0.009, 1.080, and 0.462 for $slope_2$, $angle_{23}$, F_{23}, and F_{34}, respectively. PCA was done using SPSS release 16 (SPSS Inc., Chicago, IL, USA).

2.5 Receiver Operating Characteristic (ROC) Curve Analysis

Based on staging severity, the cutoff value for the AHI was set at 5, 15, or 30. The performance of each calculated DFA plot parameter—which included the slopes of 4 segments, angles, the coordinates, as well as the surrogate variable PC1—was independently assessed using the area under the curve (AUC) of the ROC curve for different AHI cutoff values.

2.6 Statistical Analysis

Variables among and between the groups with different OSAHS severity were compared using Kruskal–Wallis and Mann–Whitney tests, respectively. Pairwise comparison of $slope_1$ and $slope_2$ was performed using Wilcoxon signed ranks test. The correlation between AHI and the DFA plot parameter was tested via the Spearman correlation coefficient. A value of $p < 0.05$ was considered statistically significant. For the ROC curve, the point with the largest sum of the sensitivity and the specificity was chosen as a cutoff in the training set. The positive and negative likelihood ratio were calculated by sensitivity/(1-specificity) and (1-sensitivity)/specificity, respectively. Classification using the cutoff value derived from ROC analysis of the training set was applied in the test set. Cross-validation in the training set was done via the "leave-one-out" method.

3 Results

Table 1 displays DFA plot parameters and PC1 of groups with different AHI severity in the training set. As the severity of sleep apnea increased, the DFA curve shifted upward and leftward at I_{23}, with a steep $slope_2$ and narrow $angle_{23}$. The moderate to severe groups had a steeper $slope_1$, flatter $slope_3$ and $slope_4$, and a greater difference between $slope_1$ and $slope_2$ than the normal to mild groups. $Slope_1$ significantly differed from $slope_2$ in each group (Wilcoxon signed ranks test, $p < 0.001$). Figure 2 demonstrates the difference between the DFA plots of a patient with severe OSAHS and a subject without OSAHS.

Table 1 Parameters of detrended fluctuation analysis according to the severity of obstructive sleep apnea–hypopnea syndrome in the training set

Severity AHI	Normal <5	Mild 5–15	Moderate 15–30	Severe >30
$Slope_1$	0.521 (0.234–0.845)[a]	0.525 (0.060–0.710)[a]	0.595 (0.094–0.884)[b]	0.732 (0.206–1.170)
$Slope_2$	0.452 (0.100–0.944)[c]	0.529 (0.100–0.885)[a]	0.764 (0.250–1.051)[b]	0.964 (0.198–1.306)
$Slope_2-slope_1$	−0.079 (−0.200 to 0.154)[c]	0.002 (−0.214 to 0.345)[a]	0.151 (−0.138 to 0.423)	0.189 (−0.290 to 0.582)
$Slope_3$	0.076 (0.032–0.485)[b]	0.082 (0.009–0.235)[a]	0.067 (0.026–0.301)[b]	0.046 (0.013–0.118)
$Slope_4$	0.045 (−0.004 to 0.295)[b]	0.052 (−0.042 to 0.198)[b]	0.049 (−0.029 to 0.482)[b]	0.038 (−0.058 to 0.163)
$Angle_{12}$	176.2 (170.8–185.0)[c]	180.1 (171.0–197.7)[b]	186.1 (173.9–197.7)	186.1 (165.2–201.8)
$Angle_{23}$	160.7 (139.1–182.9)[c]	156.7 (142.8–176.3)[b]	146.6 (135.4–168.1)[b]	139.1 (129.5–172.9)
$Angle_{34}$	178.4 (170.6–184.2)[a]	178.5 (171.3–186.7)[a]	179.3 (174.1–189.0)	179.5 (174.4–185.0)
n_{12}	1.042 (−0.256 to 8.583)	1.055 (−76.61 to 4.043)	1.042 (−9.872 to 43.47)	0.990 (−6.172 to 6.140)
F_{12}	−0.761 (−1.638 to 3.262)[c]	−0.593 (−41.72 to 1.025)[a]	−0.524 (−7.138 to 24.95)[b]	−0.441 (−6.107 to 4.252)
n_{23}	1.867 (1.711–2.337)[a]	1.878 (1.657–2.128)[a]	1.799 (1.629–2.258)[b]	1.777 (1.663–2.245)
F_{23}	−0.355 (−1.084 to −0.001)[c]	−0.174 (−1.127 to 0.279)[a]	0.022 (−0.486 to 0.375)[b]	0.333 (−0.182 to 0.793)
n_{34}	2.940 (2.267–16.63)	2.918 (2.005–3.441)	2.912 (−6.470 to 4.506)	2.935 (1.936–4.876)
F_{34}	−0.276 (−1.030 to 0.447)[c]	−0.049 (−1.091 to 0.353)[a]	0.101 (−0.424 to 0.542)[b]	0.403 (−0.129 to 0.850)
PC1	−1.283 (−2.202 to −0.085)[c]	−0.692 (−2.344 to 0.677)[c]	0.113 (−1.351 to 0.952)[c]	0.905 (−1.559 to 2.132)

Data are presented as the median with a range in parentheses

AHI apnea/hypopnea index, *PC1* surrogate variable via principal component analysis

[a] Significantly different from moderate and severe groups

[b] Significantly different from severe group

[c] Significantly different from all other groups

Table 2 Spearman correlation coefficients between the apnea/hypopnea index and parameters of the detrended fluctuation analysis plot or surrogate variable via principal component analysis

	Training set	Test set
$Slope_1$	0.61*	0.77*
$Slope_2$	0.83*	0.80*
$Slope_2-slope_1$	0.56*	0.25*
$Slope_3$	−0.51*	−0.60*
$Slope_4$	−0.26*	−0.37*
$Angle_{12}$	0.53*	0.19*
$Angle_{23}$	−0.83*	−0.81*
$Angle_{34}$	0.34*	0.29*
n_{12}	−0.20*	−0.32*
F_{12}	0.50*	0.42*
n_{23}	−0.47*	−0.57*
F_{23}	0.86*	0.83*
n_{34}	0.04[a]	0.36[a]
F_{34}	0.83*	0.81*
PC1	0.86*	0.85*

PC1 surrogate variable via principal component analysis

* $p \leq 0.001$

[a] $p > 0.05$

Table 2 shows correlations between AHI and DFA plot parameters. Table 3 shows the AUC for the ROC curves using different DFA plot parameters at three AHI cutoff values. The correlations between AHI and DFA plot parameters and the AUCs of the ROC curves were similar in the learning and test sets; both were high in $slope_2$, $angle_{23}$, F_{23}, F_{34}, and PC1.

Table 4 shows the sensitivities, specificities, predictive values, likelihood ratios, and Cohen's kappa for $slope_2$, $angle_{23}$, F_{23}, F_{34}, and PC1 in the training set. PC1 had the highest positive likelihood ratio for AHI cutoffs of 5 or 15 and the lowest negative likelihood ratio for an AHI cutoff of 30. Table 5 shows the classification results using $slope_2$, $angle_{23}$, F_{23}, F_{34}, and PC1 for 3 AHI cutoffs. The accuracies achieved by each parameter were similar among the learning set, the test set, and the cross-validated sample at different AHI cutoffs.

4 Discussion

This study presented an algorithm for parameter analyses in a DFA plot, which is a log–log plot of $F(n)$, the average fluctuation as a function of box size, against the box size n [27]. The values F_{23}, $angle_{23}$, $slope_2$, and F_{34} of the DFA plot had significant correlations with AHI and an AUC of the ROC curve $\geq$0.89 for all three AHI cutoff values. A surrogate variable, PC1, extracted via PCA had an AUC of the ROC curve >0.92 at all of the AHI cutoffs. PC1 also had the highest positive likelihood ratio for AHI cutoffs of

Table 3 Area under the curve of the receiver operating characteristic curve by detrended fluctuation analysis plot parameters for identifying obstructive sleep apnea–hypopnea syndrome subjects

AHI	Training set			Test set		
	5	15	30	5	15	30
$Slope_1$	0.71 (0.63–0.79)	0.80 (0.75–0.85)	0.83 (0.78–0.88)	0.85 (0.77–0.94)	0.83 (0.78–0.89)	0.86 (0.82–0.91)
$Slope_2$	0.89 (0.85–0.93)	0.93 (0.91–0.96)	0.91 (0.87–0.95)	0.98 (0.96–0.997)	0.94 (0.91–0.97)	0.91 (0.88–0.95)
$Slope_2-slope_1$	0.88 (0.83–0.92)	0.84 (0.80–0.89)	0.74 (0.68–0.80)	0.92 (0.87–0.97)	0.82 (0.76–0.88)	0.71 (0.64–0.78)
$-Slope_3$	0.67 (0.58–0.75)	0.74 (0.69–0.80)	0.78 (0.72–0.84)	0.72 (0.59–0.85)	0.73 (0.65–0.81)	0.82 (0.77–0.88)
$-Slope_4$	0.55 (0.45–0.65)	0.62 (0.55–0.68)	0.65 (0.59–0.72)	0.74 (0.62–0.87)	0.68 (0.60–0.77)	0.72 (0.65–0.79)
$Angle_{12}$	0.88 (0.84–0.65)	0.83 (0.79–0.88)	0.71 (0.65–0.77)	0.93 (0.88–0.98)	0.80 (0.74–0.87)	0.68 (0.61–0.76)
$-Angle_{23}$	0.89 (0.85–0.93)	0.94 (0.91–0.97)	0.91 (0.88–0.95)	0.97 (0.95–0.995)	0.93 (0.89–0.96)	0.93 (0.89–0.96)
$Angle_{34}$	0.64 (0.55–0.73)	0.69 (0.63–0.75)	0.66 (0.59–0.72)	0.58 (0.41–0.74)	0.53 (0.43–0.63)	0.63 (0.56–0.71)
$-n_{12}$	0.54 (0.44–0.63)	0.56 (0.49–0.63)	0.59 (0.52–0.66)	0.53 (0.35–0.70)	0.59 (0.49–0.69)	0.66 (0.58–0.73)
F_{12}	0.78 (0.71–0.85)	0.76 (0.71–0.82)	0.78 (0.73–0.84)	0.82 (0.73–0.92)	0.70 (0.62–0.79)	0.74 (0.67–0.81)
$-n_{23}$	0.66 (0.57–0.74)	0.75 (0.69–0.81)	0.72 (0.66–0.79)	0.55 (0.38–0.72)	0.71 (0.63–0.79)	0.78 (0.71–0.83)
F_{23}	0.92 (0.88–0.95)	0.93 (0.91–0.96)	0.93 (0.90–0.97)	0.96 (0.92–0.99)	0.90 (0.86–0.94)	0.91 (0.87–0.95)
n_{34}	0.51 (0.42–0.61)	0.53 (0.46–0.60)	0.54 (0.47–0.61)	0.54 (0.37–0.71)	0.54 (0.44–0.64)	0.50 (0.42–0.59)
F_{34}	0.89 (0.84–0.93)	0.92 (0.89–0.95)	0.92 (0.88–0.97)	0.95 (0.92–0.99)	0.89 (0.85–0.94)	0.90 (0.86–0.94)
PC1	0.92 (0.89–0.95)	0.94 (0.92–0.97)	0.93 (0.89–0.96)	0.99 (0.98–1)	0.93 (0.90–0.97)	0.93 (0.89–0.96)

Data were presented as the AUC with 95% confidence interval in parenthesis

AHI apnea/hypopnea index, *PC1* surrogate variable via principal component analysis

5 or 15 and the lowest negative likelihood ratios for an AHI cutoff of 30. The algorithm was "leave-one-out" cross-validated in the learning set and validated in the test set.

Full polysomnography is the gold standard for diagnosing OSAHS [1]. However, full polysomnography is time consuming and expensive. Alternative approaches for diagnosing sleep apnea have been developed like airflow measured by thermistor, pulse oximetry, heart rate spectral analysis and pharyngoesophageal pressure [2]. Transcutaneous nocturnal pulse oximetry increasingly is used for initially screening for OSAHS, as it is inexpensive, simply performed, and easily interpreted [4]. The sensitivity of nocturnal pulse oximetry in diagnosing OSAHS is 31–98% with a specificity of 41–100% [36]. Because the SaO_2 data recorded in sleep is a time series that fluctuates considerably, variability tests such as delta index [3] and spectral analysis [31, 37] are valuable for identifying OSAHS subjects.

The DFA method of variability analysis is advantageous because it identifies intrinsic variation in the physiologic system and does not require a stationary signal series [17, 27]. This work developed an algorithm using a free statistical package, R, to analyze the DFA log–log plot. The derived parameters demonstrated good diagnostic performances in identifying OSAHS. The largest AUCs of the ROC curve for different AHI cutoff values were 0.92 by PC1 and F_{23} for 5; 0.94 by PC1 and $angle_{23}$ for 15; and 0.93 by PC1 and F_{23} for 30. The results were validated by polysomnographic study in a different group of subjects, demonstrating that DFA plot parameters are useful for identifying OSAHS.

In patients with severe heart failure, the scaling exponent α of the cardiac interbeat interval, which is the slope of the line relating log $F(n)$ to log n, differs from that of normal subjects [27]. The α exponent derived from a small n ($n < 10$; equivalent to $slope_1$) is larger than that from a large n ($n > 10$; close to $slope_2$) in normal subjects, and the converse is true in heart failure patients. A similar phenomenon was observed in a comparison of the α exponent derived from the DFA analysis of SpO_2 data in normal and sleep apnea subjects. Normal subjects and patients with mildly severe sleep apnea had α exponents ($slope_1$ and $slope_2$) close to 0.5, which suggests a random walk and that the value of one SpO_2 is unlikely to correlate with that immediately before it. In contrast, patients with moderate to severe sleep apnea had α exponents between 0.5 and 1, indicating a higher-than-average value of SpO_2 likely to be followed by a high SpO_2, and vice versa [27]. The decrement and increment of SpO_2 during desaturation and resaturation caused by apnea/hypopnea events produced high α exponents ($slope_1$ and $slope_2$) in the moderate to severe group. Flat $slope_3$ and $slope_4$ suggest that the fluctuation invoked by the apnea/hypopnea event is episodic and short in duration, and its effects on $F(n)$ are diluted by long SpO_2 data segments with less variability in the flanking region of acute desaturation and resaturation, when the size of the box is large.

Table 4 Usefulness of detrended fluctuation analysis plot parameters in the diagnosis of obstructive sleep apnea–hypopnea syndrome in the training set

	$Slope_2$			$-Angle_{23}$			F_{23}			F_{34}			PC1		
AHI cutoff	5	15	30	5	15	30	5	15	30	5	15	30	5	15	30
Cutoff	0.533	0.697	0.761	−155.7	−147.5	−147.0	−0.182	−0.017	0.055	−0.095	0.122	0.122	−0.785	−0.059	0.0004
Sensitivity	83	86	88	81	79	90	84	85	91	85	77	92	83	77	94
Specificity	89	94	80	92	97	80	89	90	84	87	94	79	92	98	79
PV+	98	96	75	98	98	76	98	93	80	98	96	75	98	98	75
PV−	45	80	91	44	74	92	48	79	93	49	72	93	47	73	95
LR+	7.84	15	4.33	10.3	27.7	4.56	8.00	8.94	5.67	6.47	13.5	4.38	10.57	40.63	4.46
LR−	0.195	0.152	0.147	0.203	0.214	0.123	0.176	0.164	0.107	0.172	0.24	0.103	0.18	0.231	0.08
Kappa	0.51	0.78	0.65	0.50	0.72	0.68	0.54	0.68	0.73	0.54	0.68	0.69	0.54	0.71	0.70

AHI apnea/hypopnea index, *LR+* positive likelihood ratio, *LR−* negative likelihood ratio, *PC1* surrogate variable via principal component analysis, *PV+* positive predictive value, *PV−* negative predictive value, *kappa* Cohen's kappa

Table 5 Classification results at different apnea/hypopnea index cutoffs

	$Slope_2$			$-Angle_{23}$			F_{23}			F_{34}			PC1		
AHI cutoff	5	15	30	5	15	30	5	15	30	5	15	30	5	15	30
Accuracy (%)															
Training set	89	87.2	84.6	82.8	86.1	84.2	85.0	87.2	86.4	85.3	83.9	84.2	85	88.6	85
Cross-validated[a]	88.6	86.8	84.6	82.1	79.9	81.0	84.2	86.4	86.4	85.0	82.4	83.9	84.2	88.3	84.6
Test set	95.1	85.4	82.5	86.9	78.2	87.4	90.8	84.0	85.9	89.3	80.6	83.5	90.8	80.1	87.4

AHI apnea/hypopnea index, *PC1* surrogate variable via principal component analysis

[a] "Leave-one-out" cross-validation in the training set

Table 6 Performances of different classification algorithms on oxyhemoglobin saturation by pulse oximetry in predicting obstructive sleep apnea–hypopnea syndrome

Author	Morillo et al. [38]	Marcos et al. [39]	Gutiérrez-Tobal et al. [40]	Morillo et al. [41]	Álvarez et al. [42]	Hang et al. [43]	Current study
Method	Multiclass classification	Kernel entropy	Multi-class AdaBoost	Frequency desaturation index	Feature selection by genetic algorithm	Frequency domain index	Detrended fluctuation analysis (PC1)
Number of subjects[a]	117|-	96|144	192|128	37|78	96|144	257/279	273|206
Cross-validation	Loocv	Hold-out	Hold-out	Hold-out	Hold-out	Hold-out	Loocv|hold-out
Accuracy/%[b]	82.6	–	89.8/85.8/74.8	–	87.5	–	84.2/88.3/84.6 |90.8/80.1/87.4
AUC[a]	0.9|-	0.86|0.91	–	–|0.89/0.9/0.91/0.92	–	0.93/0.96|	0.92/0.94/0.93
						0.91/0.94	|0.99/0.93/0.93
AHI cutoff	5/15/30	10	5/15/30	5/10/15/20	10	15/30	5/15/30

Loocv leave-one-out cross-validation, *PC1* surrogate variable via principal component analysis

[a] Training set\|test set

[b] Accuracy by loocv in training set or cross-validation in test set

The characteristics of crossover on the DFA plot are affected by the presence of random spikes or segments with different local behavior in the signals [30]. The AHI measures the frequency of disordered breathing events, which cause oxyhemoglobin desaturation [1]. This study revealed that AHI is significantly correlated with $slope_2$, $angle_{23}$, and F_{23}, which are all related to the curved crossover. The DFA plot had a curve with steep $slope_2$, narrow $angle_{23}$, and an upward shift in the presence of large AHI. Superposition [30] of the scaling of the underlying sinusoidal trend and the scaling of the spikes evoked by apnea/hypopnea events may give the DFA plot of SpO_2 signals its appearance.

The diagnostic performance was similar to the performance of several automated algorithms on oxyhemoglobin saturation alone with a single AHI cutoff of 10 or 15 [5–10] and comparable to those of recent developed ones (Table 6) [38–43]. This study provides data at different AHI cutoffs that correspond to the severity of OSAHS and have a large number of subjects in both the learning and test sets.

5 Conclusion

This study demonstrated that parameters derived from the DFA plot, especially the curved crossover, correlate significantly with AHI and perform well in diagnosing OSAHS. Further study in the ambulatory setting is needed to validate the usefulness of DFA plots in screening OSAHS patients. The algorithm should further be tested on non-obstructive sleep-related breathing disorders such as central apnea or OSAHS with a coexisting lung dysfunction, such as in chronic obstructive pulmonary disease. Further work is also needed to clarify the impacts of sleep state change and fragmentation of sleep architecture on the DFA plot of SpO_2 during sleep.

References

1. Caples, S. M., Gami, A. S., & Somers, V. K. (2005). Obstructive sleep apnea. *Annals of Internal Medicine, 142*(3), 187–197.
2. Flemons, W. W., Littner, M. R., Rowley, J. A., Gay, P., Anderson, W. M., Hudgel, D. W., et al. (2003). Home diagnosis of sleep apnea: A systematic review of the literature. An evidence review cosponsored by the American Academy of Sleep Medicine, the American College of Chest Physicians, and the American Thoracic Society. *Chest, 124*(4), 1543–1579.
3. Magalang, U. J., Dmochowski, J., Veeramachaneni, S., Draw, A., Mador, M. J., El-Solh, A., et al. (2003). Prediction of the apnea-hypopnea index from overnight pulse oximetry. *Chest, 124*(5), 1694–1701.
4. Bennett, J. A., & Kinnear, W. J. (1999). Sleep on the cheap: the role of overnight oximetry in the diagnosis of sleep apnoea hypopnoea syndrome. *Thorax, 54*(11), 958–959.

5. Marcos, J. V., Hornero, R., Alvarez, D., Del Campo, F., & Aboy, M. (2010). Automated detection of obstructive sleep apnoea syndrome from oxygen saturation recordings using linear discriminant analysis. *Medical and Biological Engineering and Computing, 48*(9), 895–902.
6. Marcos, J. V., Hornero, R., Alvarez, D., del Campo, F., Lopez, M., & Zamarron, C. (2008). Radial basis function classifiers to help in the diagnosis of the obstructive sleep apnoea syndrome from nocturnal oximetry. *Medical and Biological Engineering and Computing, 46*(4), 323–332.
7. Marcos, J. V., Hornero, R., Alvarez, D., del Campo, F., & Zamarron, C. (2009). Assessment of four statistical pattern recognition techniques to assist in obstructive sleep apnoea diagnosis from nocturnal oximetry. *Medical Engineering & Physics, 31*(8), 971–978.
8. Marcos, J. V., Hornero, R., Alvarez, D., Del Campo, F., Zamarron, C., & Lopez, M. (2008). Utility of multilayer perceptron neural network classifiers in the diagnosis of the obstructive sleep apnoea syndrome from nocturnal oximetry. *Computer Methods and Programs in Biomedicine, 92*(1), 79–89.
9. Marcos, J. V., Hornero, R., Alvarez, D., Nabney, I. T., Del Campo, F., & Zamarron, C. (2010). The classification of oximetry signals using Bayesian neural networks to assist in the detection of obstructive sleep apnoea syndrome. *Physiological Measurement, 31*(3), 375–394.
10. Morillo, D. S., Rojas, J. L., Crespo, L. F., Leon, A., & Gross, N. (2009). Poincare analysis of an overnight arterial oxygen saturation signal applied to the diagnosis of sleep apnea hypopnea syndrome. *Physiological Measurement, 30*(4), 405–420.
11. Zamarron, C., Gude, F., Barcala, J., Rodriguez, J. R., & Romero, P. V. (2003). Utility of oxygen saturation and heart rate spectral analysis obtained from pulse oximetric recordings in the diagnosis of sleep apnea syndrome. *Chest, 123*(5), 1567–1576.
12. Alvarez, D., Hornero, R., Abasolo, D., del Campo, F., Zamarron, C., & Lopez, M. (2009). Nonlinear measure of synchrony between blood oxygen saturation and heart rate from nocturnal pulse oximetry in obstructive sleep apnoea syndrome. *Physiological Measurement, 30*(9), 967–982.
13. de Chazal, P., Heneghan, C., & McNicholas, W. T. (2009). Multimodal detection of sleep apnoea using electrocardiogram and oximetry signals. *Philosophical Transactions of the Royal Society of London A, 367*(1887), 369–389.
14. Heneghan, C., Chua, C. P., Garvey, J. F., de Chazal, P., Shouldice, R., Boyle, P., et al. (2008). A portable automated assessment tool for sleep apnea using a combined Holter-oximeter. *Sleep, 31*(10), 1432–1439.
15. Narkiewicz, K., van de Borne, P. J., Pesek, C. A., Dyken, M. E., Montano, N., & Somers, V. K. (1999). Selective potentiation of peripheral chemoreflex sensitivity in obstructive sleep apnea. *Circulation, 99*(9), 1183–1189.
16. Suki, B. (2002). Fluctuations and power laws in pulmonary physiology. *American Journal of Respiratory and Critical Care Medicine, 166*(2), 133–137.
17. Seely, A. J., & Macklem, P. T. (2004). Complex systems and the technology of variability analysis. *Critical Care, 8*(6), R367–R384.
18. Makikallio, T. H., Koistinen, J., Jordaens, L., Tulppo, M. P., Wood, N., Golosarsky, B., et al. (1999). Heart rate dynamics before spontaneous onset of ventricular fibrillation in patients with healed myocardial infarcts. *The American Journal of Cardiology, 83*(6), 880–884.
19. Tapanainen, J. M., Thomsen, P. E., Kober, L., Torp-Pedersen, C., Makikallio, T. H., Still, A. M., et al. (2002). Fractal analysis of heart rate variability and mortality after an acute myocardial infarction. *The American Journal of Cardiology, 90*(4), 347–352.
20. Laitio, T. T., Huikuri, H. V., Kentala, E. S., Makikallio, T. H., Jalonen, J. R., Helenius, H., et al. (2000). Correlation properties and complexity of perioperative RR-interval dynamics in coronary artery bypass surgery patients. *Anesthesiology, 93*(1), 69–80.
21. Laitio, T. T., Huikuri, H. V., Makikallio, T. H., Jalonen, J., Kentala, E. S., Helenius, H., et al. (2004). The breakdown of fractal heart rate dynamics predicts prolonged postoperative myocardial ischemia. *Anesthesia and Analgesia, 98*(5), 1239–1244.
22. Ho, K. K., Moody, G. B., Peng, C. K., Mietus, J. E., Larson, M. G., Levy, D., et al. (1997). Predicting survival in heart failure case and control subjects by use of fully automated methods for deriving nonlinear and conventional indices of heart rate dynamics. *Circulation, 96*(3), 842–848.
23. Varela, M., Churruca, J., Gonzalez, A., Martin, A., Ode, J., & Galdos, P. (2006). Temperature curve complexity predicts survival in critically ill patients. *American Journal of Respiratory and Critical Care Medicine, 174*(3), 290–298.
24. Hwa, R. C., & Ferree, T. C. (2002). Scaling properties of fluctuations in the human electroencephalogram. *Physical Review E: Statistical, Nonlinear, and Soft Matter Physics, 66*(2 Pt 1), 021901.
25. Stam, C. J., Montez, T., Jones, B. F., Rombouts, S. A., van der Made, Y., Pijnenburg, Y. A., et al. (2005). Disturbed fluctuations of resting state EEG synchronization in Alzheimer's disease. *Clinical Neurophysiology, 116*(3), 708–715.
26. Goldberger, A. L., Amaral, L. A., Hausdorff, J. M., Ivanov, P., Peng, C. K., & Stanley, H. E. (2002). Fractal dynamics in physiology: alterations with disease and aging. *Proceedings of National Academic Science U S A, 99*(Suppl 1), 2466–2472.
27. Peng, C. K., Havlin, S., Stanley, H. E., & Goldberger, A. L. (1995). Quantification of scaling exponents and crossover phenomena in nonstationary heartbeat time series. *Chaos, 5*(1), 82–87.
28. Makikallio, T. H., Ristimae, T., Airaksinen, K. E., Peng, C. K., Goldberger, A. L., & Huikuri, H. V. (1998). Heart rate dynamics in patients with stable angina pectoris and utility of fractal and complexity measures. *The American Journal of Cardiology, 81*(1), 27–31.
29. Huikuri, H. V., Makikallio, T. H., Peng, C. K., Goldberger, A. L., Hintze, U., & Moller, M. (2000). Fractal correlation properties of R–R interval dynamics and mortality in patients with depressed left ventricular function after an acute myocardial infarction. *Circulation, 101*(1), 47–53.
30. Chen, Z., Ivanov, P., Hu, K., & Stanley, H. E. (2002). Effect of nonstationarities on detrended fluctuation analysis. *Physical Review E: Statistical, Nonlinear, and Soft Matter Physics, 65*(4 Pt 1), 041107.
31. Hua, C. C., & Yu, C. C. (2007). Smoothed Periodogram of oxyhemoglobin saturation by pulse oximetry in sleep apnea syndrome: An automated analysis. *Chest, 131*(3), 750–757.
32. Hu, K., Ivanov, P. C., Chen, Z., Carpena, P., & Stanley, H. E. (2001). Effect of trends on detrended fluctuation analysis. *Physical Review E: Statistical, Nonlinear, and Soft Matter Physics, 64*(1 Pt 1), 011114.
33. Venables, W. N., & Ripley, B. D. (2002). *Modern applied statistics with S* (4th ed.). New York: Springer-Verlag.
34. R Development Core & Team. (2010). *R: A language and environment for statistical computing*. Vienna, Austria: R Foundation for Statistical Computing.
35. Hair, J. F., Black, W. C., Babin, B. J., & Anderson, R. E. (2010). *Multivariate data analysis: A global perspective*. Upper Saddle River: Pearson Education Inc.
36. Schlosshan, D., & Elliott, M. W. (2004). Sleep. 3: Clinical presentation and diagnosis of the obstructive sleep apnoea hypopnoea syndrome. *Thorax, 59*(4), 347–352.

37. Zamarron, C., Romero, P. V., Rodriguez, J. R., & Gude, F. (1999). Oximetry spectral analysis in the diagnosis of obstructive sleep apnoea. *Clinical science (London, England), 97*(4), 467–473.
38. Sánchez-Morillo, D., López-Gordo, M., & León, A. (2014). Novel multiclass classification for home-based diagnosis of sleep apnea hypopnea syndrome. *Expert Systems with Applications, 41*(4), 1654–1662.
39. Marcos, J. V., Hornero, R., Nabney, I. T., Álvarez, D., Gutiérrez-Tobal, G. C., & del Campo, F. (2016). Regularity analysis of nocturnal oximetry recordings to assist in the diagnosis of sleep apnoea syndrome. *Medical Engineering & Physics, 38*(3), 216–224.
40. Gutiérrez-Tobal, G., Álvarez, D., Crespo, A., Arroyo, C., Vaquerizo-Villar, F., Barroso-García, V., et al. (2016). Multiclass adaboost to detect Sleep Apnea-Hypopnea Syndrome severity from oximetry recordings obtained at home. In *2016 Global Medical Engineering Physics Exchanges/Pan American Health Care Exchanges (GMEPE/PAHCE), 2016* (pp. 1–5): IEEE
41. Morillo, D. S., Gross, N., León, A., & Crespo, L. F. (2012). Automated frequency domain analysis of oxygen saturation as a screening tool for SAHS. *Medical Engineering & Physics, 34*(7), 946–953.
42. Álvarez, D., Hornero, R., Marcos, J. V., & del Campo, F. (2012). Feature selection from nocturnal oximetry using genetic algorithms to assist in obstructive sleep apnoea diagnosis. *Medical Engineering & Physics, 34*(8), 1049–1057.
43. Hang, L.-W., Yen, C.-W., & Lin, C.-L. (2012). Frequency-domain index of oxyhemoglobin saturation from pulse oximetry for obstructive sleep apnea syndrome. *Journal of Medical and Biological Engineering, 32*(5), 343–348.